



**Evidence for Karyogamy and Exchange of Genetic Material in the Binucleate Intestinal Parasite *Giardia intestinalis***

Marianne K. Poxleitner, *et al.*  
*Science* **319**, 1530 (2008);  
DOI: 10.1126/science.1153752

***The following resources related to this article are available online at [www.sciencemag.org](http://www.sciencemag.org) (this information is current as of March 23, 2008 ):***

**Updated information and services**, including high-resolution figures, can be found in the online version of this article at:

<http://www.sciencemag.org/cgi/content/full/319/5869/1530>

**Supporting Online Material** can be found at:

<http://www.sciencemag.org/cgi/content/full/319/5869/1530/DC1>

This article **cites 16 articles**, 9 of which can be accessed for free:

<http://www.sciencemag.org/cgi/content/full/319/5869/1530#otherarticles>

This article appears in the following **subject collections**:

Genetics

<http://www.sciencemag.org/cgi/collection/genetics>

Information about obtaining **reprints** of this article or about obtaining **permission to reproduce this article** in whole or in part can be found at:

<http://www.sciencemag.org/about/permissions.dtl>

*CYP79B3* and *CYP79B2* (9, 11). The encoded proteins catalyze the conversion of tryptophan into indole-3-acetaldoxime in tryptophan-dependent auxin biosynthesis in *Arabidopsis* (12–14). In tomato, overexpression of *SUN* resulted in extremely elongated and often seedless fruit, reminiscent of the parthenocarpic, elongated, and pointed tomato fruit resulting from expression of the auxin biosynthesis gene *iaaM* controlled by the placenta and ovule-specific *DefH9* promoter (15, 16). The extremely elongated fruit shape and lack of proper seed development when *SUN* is overexpressed, in addition to its potential biochemical function, suggest that *SUN* may affect auxin levels or distribution in the fruit (Fig. 3E). It is therefore plausible that involvement of *SUN* in shape variation is through regulation of plant hormone and/or secondary metabolite levels, thereby affecting the patterning of the fruit.

#### References and Notes

- J. F. Doebley, B. S. Gaut, B. D. Smith, *Cell* **127**, 1309 (2006).
- I. Paran, E. van der Knaap, *J. Exp. Bot.* **58**, 3841 (2007).
- E. van der Knaap, S. D. Tanksley, *Theor. Appl. Genet.* **103**, 353 (2001).
- E. van der Knaap, A. Sanyal, S. A. Jackson, S. D. Tanksley, *Genetics* **168**, 2127 (2004).
- S. Abel, T. Savchenko, M. Levy, *BMC Evol. Biol.* **5**, 72 (2005).
- K. Lertpiriyapong, Z. R. Sung, *Plant Mol. Biol.* **53**, 581 (2003).
- A. Majira, M. Domin, O. Grandjean, K. Gofron, N. Houba-Herlin, *Plant Mol. Biol.* **50**, 551 (2002).
- S. Takada, K. Hibara, T. Ishida, M. Tasaka, *Development* **128**, 1127 (2001).
- M. Levy, Q. Wang, R. Kaspi, M. P. Parrella, S. Abel, *Plant J.* **43**, 79 (2005).
- B. Lewin, *Genes IX* (Jones and Bartlett, Sudbury, MA, ed. 9, 2008).
- C. D. Grubb, S. Abel, *Trends Plant Sci.* **11**, 89 (2006).
- A. K. Hull, R. Vij, J. L. Celenza, *Proc. Natl. Acad. Sci. U.S.A.* **97**, 2379 (2000).
- M. D. Mikkelsen, C. H. Hansen, U. Wittstock, B. A. Halkier, *J. Biol. Chem.* **275**, 33712 (2000).

- Y. Zhao *et al.*, *Genes Dev.* **16**, 3100 (2002).
- N. Ficcidenti *et al.*, *Mol. Breed.* **5**, 463 (1999).
- T. Pandolfini, G. L. Rotino, S. Camerini, R. Defez, A. Spena, *BMC Biotechnol.* **2**, 1 (2002).
- We thank T. Meulia and A. Kaszas at the Molecular and Cellular Imaging Center in Wooster for microscopy and sequencing, as well as D. Francis, S. Kamoun, D. Mackey, and P. Springer for comments. This work was funded in part by NSF: DBI 0227541 and DBI 0400811 (to E.v.d.K.); DBI 0110124 (to E.J.S.). Accession numbers of deposited sequences: EF094939, EF094940, EF094941, and EU491503.

#### Supporting Online Material

www.sciencemag.org/cgi/content/full/319/5869/1527/DC1  
Materials and Methods  
SOM Text  
Figs. S1 to S7  
Tables S1 to S4  
References

15 November 2007; accepted 8 February 2008  
10.1126/science.1153040

## Evidence for Karyogamy and Exchange of Genetic Material in the Binucleate Intestinal Parasite *Giardia intestinalis*

Marianne K. Poxleitner,<sup>1\*</sup> Meredith L. Carpenter,<sup>1\*</sup> Joel J. Mancuso,<sup>1</sup> Chung-Ju R. Wang,<sup>1</sup> Scott C. Dawson,<sup>2</sup> W. Zacheus Cande<sup>1†</sup>

The diplomonad parasite *Giardia intestinalis* contains two functionally equivalent nuclei that are inherited independently during mitosis. Although presumed to be asexual, *Giardia* has low levels of allelic heterozygosity, indicating that the two nuclear genomes may exchange genetic material. Fluorescence in situ hybridization performed with probes to an episomal plasmid suggests that plasmids are transferred between nuclei in the cyst, and transmission electron micrographs demonstrate fusion between cyst nuclei. Green fluorescent protein fusions of giardial homologs of meiosis-specific genes localized to the nuclei of cysts, but not the vegetative trophozoite. These data suggest that the fusion of nuclei, or karyogamy, and subsequently somatic homologous recombination facilitated by the meiosis gene homologs, occur in the giardial cyst.

*Giardia intestinalis* (syn. *lamblia*, *duodenalis*) is a common intestinal protozoan parasite and a major cause of water-borne diarrheal disease worldwide (1). As a diplomonad, it has two apparently genetically identical, functionally equivalent diploid nuclei (2–4), and the sequenced genome shows little heterozygosity (5, 6). Both nuclei are transcriptionally active and contain two complete copies of the genome (2–4). The parasite has two developmental stages: a binucleate, flagellated trophozoite that attaches to the upper small intestine, and the quadrinucleate infectious cyst, which is excreted from the body and persists in the water supply (7). In the encysting trophozoite, the two nuclei are thought to

undergo a nuclear division without a subsequent cytokinesis, giving rise to a mature cyst with four nuclei (8). Upon excystation, the cell goes through one cellular division and then one nuclear and cellular division to form four binucleate trophozoites (8).

The two nuclei in the trophozoite remain physically and genetically distinct during mitosis, with two autonomous spindles segregating the parental nuclei into the daughter cells (9). Neither mating nor meiosis has been reported in *Giardia*. However, if *Giardia* is asexual, it should accumulate substantial allelic heterozygosity within and between the two nuclei, and this has not been observed (5, 6, 10).

To determine whether the cyst nuclei remain physically autonomous, as they do in trophozoites, or whether nuclei can exchange genetic material, we performed fluorescent in situ hybridization (FISH) on trophozoites and cysts (9). In *Giardia*, stably transfected plasmids (episomes) are found in only one of the two nuclei

of trophozoites (Fig. 1A). This pattern persists throughout cell division and cytokinesis (9, 11). When we use FISH to detect episomes in cysts, we see two distinct patterns ( $n = 50$ ): 72% of the cysts have several episomes present in two of the four nuclei (Fig. 1B), whereas 28% of the cysts have episomes in three of the four nuclei (Fig. 1C). This result suggests that in roughly one-third of encysting cells, two nuclei come together and their nuclear envelopes fuse, resulting in plasmid transfer between the nuclei.

To ascertain whether nuclear fusion occurs in *Giardia* cysts, we performed transmission electron microscopy (TEM). Cysts were prepared for TEM with high-pressure rapid freezing–freeze substitution to achieve optimal cytological preservation and eliminate chemical fixation artifacts due to the impermeability of the cyst wall. Using this method, we observed nuclei joined by contiguous membranes (Fig. 1, D and E). These nuclear envelope (NE) fusion morphologies are not derived from an incomplete mitosis because there are no spindle microtubules associated with the NE, and the multiple axonemes associated with paired and fusing nuclei differ in location from the axoneme pairs found at each spindle pole in mitotic cells (9). Of the ~100 individual cysts examined, we observed 15 with contiguous NEs. Because these cells were collected at a single moment in time, the percentage of nuclear fusions is less than that seen by FISH, which represents the net outcome of nuclear fusions over time. Thus, the nuclei in the *Giardia* cyst fuse (undergo karyogamy), and this fusion likely facilitates the transfer of episomes between nuclei.

We next sought to determine when karyogamy takes place in the encystation process. We counted the number of nuclei in cysts and the total number of cysts present at six different time points (Fig. 2A). Cysts appeared 12 hours after induction of encystation; subsequently, multiple nuclear arrangements were seen in cysts at every time point, suggesting that encystation is not well synchronized and that cells at varying stages of

<sup>1</sup>Department of Molecular and Cell Biology, University of California, Berkeley, CA 94720, USA. <sup>2</sup>Section of Microbiology, 255 Briggs Hall, One Shields Avenue, University of California, Davis, CA 95616, USA.

\*These authors contributed equally to this work.

†To whom correspondence should be addressed. E-mail: zcande@berkeley.edu

encystation are always present. Three nuclear arrangements could be distinguished at intermediate time points: two pairs of nuclei at opposite ends of the cell, two pairs of nuclei close together, and three nuclei (a pair of nuclei and one large chromatin mass) usually close together (Fig. 2A).

Cysts with four nuclei close together were always the most abundant. These data are consistent with the hypothesis that at the four-nuclear stage, the nuclear pairs migrate from opposite ends of the cell to the same quadrant, undergo fusion, and then separate again.

Time-lapse images of live, acridine orange–stained cysts illustrate this dynamic nuclear behavior (Fig. 2, B to G and movies S1 to 3). Each nuclear pair exhibits two forms of movement (Fig. 2, B to G). The pair on the right moves relative to the pair on the left, and in 32 s rotates from a horizontal (Fig. 2B) to a vertical (Fig. 2F) orientation. The nuclei within each pair also fluctuate back and forth (Fig. 2, B to G). The nuclear movements in cysts are very different from what is observed in trophozoites, in which the two nuclei are tethered to the cytoskeleton and exhibit no movement (movie S2) except during mitosis. The dynamic movements of cyst nuclei may provide the force necessary for karyogamy to occur and promote mixing of nuclear contents.

To determine how plasmid distribution changes relative to nuclear configuration, FISH was performed on encysting cultures to detect transfected plasmids (Fig. 2, H to L). As in Fig. 1, trophozoites contained plasmids in only one of the two nuclei (Fig. 2H). In 32% of cysts ( $n = 50$ ), two nuclear pairs were present at opposite ends of the cell, with plasmids in one nucleus of each pair (Fig. 2I). In 21% of cysts, two nuclear pairs were present together at the same end of the cell, with plasmids in one nucleus of each pair (Fig. 2J). In both of these categories (Fig. 2, I and J), plasmids were detected in only one nucleus in each pair, indicating that the pairs are nondaughters (derived from different parental nuclei). In 19% of cysts, three nuclei were present, presumably in the process of fusion, with plasmids in two of the three nuclei (Fig. 2K). Finally, in 27% of cysts, plasmids were seen in three of the four paired nuclei (Fig. 2L). Because all of these configurations appear at roughly the same time, the processes of nuclear migration, fusion, plasmid exchange, and fission may occur very quickly.

Cysts were immunolabeled with antibodies to  $\alpha$ -tubulin to identify major microtubule arrays associated with cyst nuclei. Again, we saw three major classes of encysting cells: two pairs of nuclei far apart, two pairs close together, and

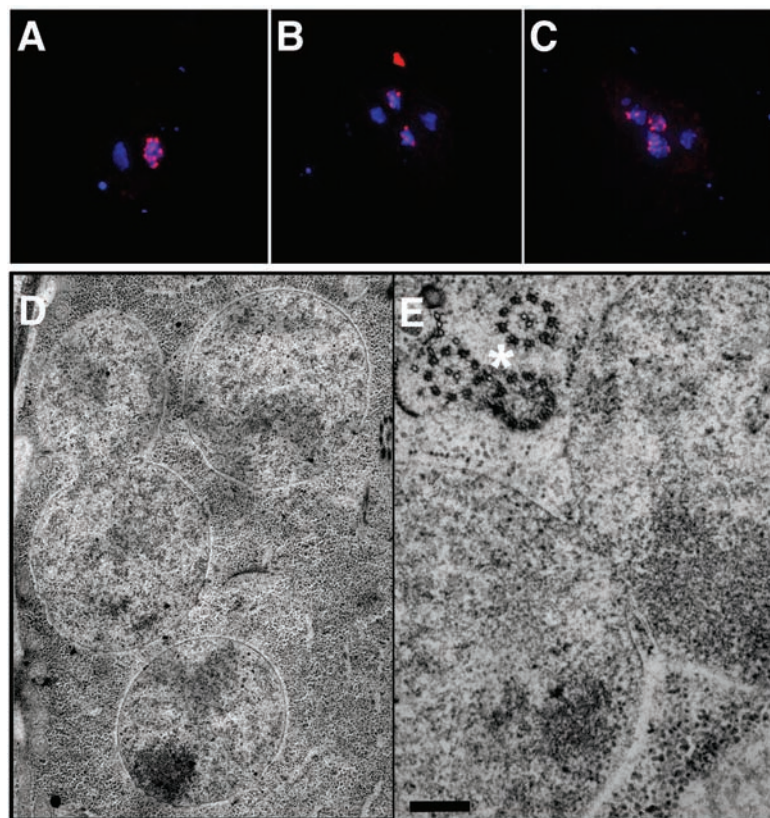
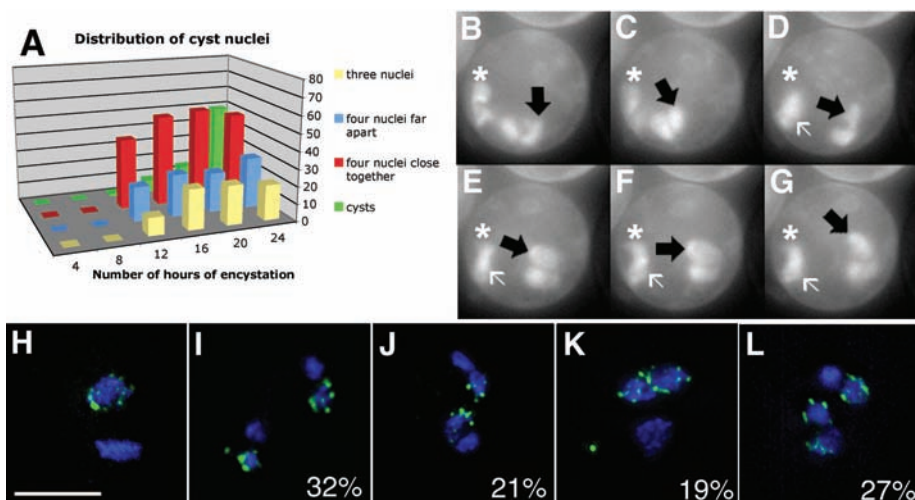


**Fig. 1.** Plasmids detected by FISH in *Giardia* trophozoites and cysts, and TEM showing nuclear fusion (karyogamy) in cysts. (A) When FISH is performed on trophozoites containing transformed plasmids, plasmid probes (red spots) are detected in only one of the two 4', 6'-diamidino-2-phenylindole (DAPI)-stained (blue) nuclei. (B and C) In cysts, plasmid probes are seen in either two of the four nuclei (B) or three of the four nuclei (C). (D) TEM image of a mature cyst. All four cyst nuclei are in the same plane; two of the nuclei are fused with contiguous nuclear envelopes. (E) Two fused nuclei from a different cell. Cytoplasmic axonemes are marked with an asterisk. Bar, 200 nm.

**Fig. 2.** Nuclear movements and plasmid distribution in *Giardia* cysts. (A) Time course of nuclear number and position during encystation. (B to G) Selected frames 8 s apart from a movie of a live, acridine orange–stained cyst. The black arrow follows the movement of the nuclear pair on the right side of the cyst. The nuclei within each pair also oscillate [asterisk in (B) to (G)]. The possible fusion of the left pair of nuclei is indicated by a white arrow in (D) to (G). Also see movies S1 to S3 (11). (H to L) Nuclear configuration and plasmid distribution. (H) In trophozoites, the plasmids (green spots) are detected by FISH in only one of the two nuclei. (I) Plasmids are detected in two of the four cyst nuclei when the two nuclear pairs are far apart. (J) Plasmids are detected in two of the four nuclei and the two nuclear pairs are close together. (K) Cyst nuclei have presumably undergone fusion, and plasmids are detected in two of the three nuclei. (L) Plasmids are present in three of the four nuclei. Percentages of each class of cyst are indicated in (I) to (L). Bar, 5  $\mu$ m.



three nuclei (Fig. 3, A to C). Three-dimensional projections of these images (movies S4 to S6) demonstrate that the three nuclei seen in Fig. 3C are indeed three separate nuclei and not two nuclei superimposed on one another. The cyst microtubule cytoskeleton differs from the trophozoite cytoskeleton, because many of the complex structures seen in trophozoites are absent in the cyst (Fig. 3, A to C). Disassembled fragments of the ventral disk and internal axonemes are prominent (Fig. 3B). As shown by TEM (Fig. 1E) and immunofluorescence (Fig. 3, A to C), the nuclear pairs are associated with microtubule bundles, especially internal axonemes, throughout cyst formation, suggesting that the axonemes may have a distinctive function in *Giardia*.

On the basis of these data, we propose a model for plasmid transfer during encystation (Fig. 3D). First, at the induction of encystation, the nuclei divide with two separate spindles. This division generates a cyst with two pairs of non-daughter nuclei at opposite ends of the cell. Each pair of nuclei appears to be associated with a bundle of internal axonemes and moves together within the cyst (Figs. 1E and 2, B to G). One pair of nuclei then migrates to the opposite end of the cell to join the other nuclear pair. At some point, karyogamy between two non-daughter nuclei can occur, resulting in the appearance of three nuclei. This three-nuclear stage is commonly observed with all three nuclei in close proximity to one another, so the actual fusion probably occurs after the nuclei have migrated together at one end of the cell. Because we have never seen plasmids in all four nuclei of cysts, we conclude that fusion is typically restricted to only one set of nuclei. Alternatively, fusion may occur between both pairs of non-daughter nuclei, but may only occasionally result in genetic exchange. If fusion were occurring between daughter nuclei, it would not be detected as an increase in number of labeled nuclei in our FISH experiments. Finally, because fully mature cysts have four nuclei before excystation, we deduce that nuclear fission and the re-formation of four separate nuclei must follow karyogamy and nucleoplasm exchange.

For karyogamy to lead to genome homogenization, we assume that an event like homologous recombination occurs after the nuclear envelopes fuse. Thus, we predict that the expression of genes involved in DNA repair and/or homologous recombination should increase during encystation. Although meiosis has not been described in *Giardia*, analysis of its sequenced genome revealed homologs of meiosis-specific genes (HMGs), including Hop1, Spo11, Dmc1a, Dmc1b, and Mnd1 (5, 12). Nonetheless, it is possible that these genes had a nonmeiotic function in the last common ancestor of *Giardia* and other eukaryotes; indeed, many researchers believe that the eukaryotic meiosis machinery originally evolved from genes involved in DNA damage repair (13). The HMGs in *Giardia* may therefore facilitate the exchange of genomic

material within and between the cell's two nuclear genomes after karyogamy.

To assess the expression and localization of the protein products of HMGs, we constructed C-terminal green fluorescent protein (GFP) fusion constructs of these five genes under their native promoters. We observed DMC1A::GFP localization to the four cyst nuclei (fig. S1, A to C). However, no GFP was visible in the nuclei of the trophozoites (fig. S1, D to F). This same pattern was seen for SPO11::GFP (fig. S2, A and B) and HOP1::GFP (see below). In contrast, DMC1B::GFP (fig. S1, G to L) and MND1::GFP (fig. S2, C and D) localize to the nuclei of both trophozoites and cysts. Interestingly, although *Giardia* contains two putative homologs of the meiosis-specific RecA family member Dmc1, no homologs of Rad51, the somatic and meiotic

**Fig. 4.** The timing of HOP1::GFP expression during encystation. After 3 hours (A) of exposure to encystation conditions, no HOP1::GFP (green) is detected, but immunolabeling with antibodies to CWP (red) shows a small amount of CWP present in ESVs. After 12 hours of encystation (B), the amount of CWP detected in ESVs has increased, but no HOP1::GFP is visible. By 15 hours (C), HOP1::GFP is detected and colocalizes to two DAPI (blue)-stained nuclei, while the cell is filled with vesicles containing CWP. When encystation is complete at 24 hours (D), HOP1::GFP is seen in the four-cyst nuclei, and the cyst wall is smooth and contiguous around the periphery of the cell.

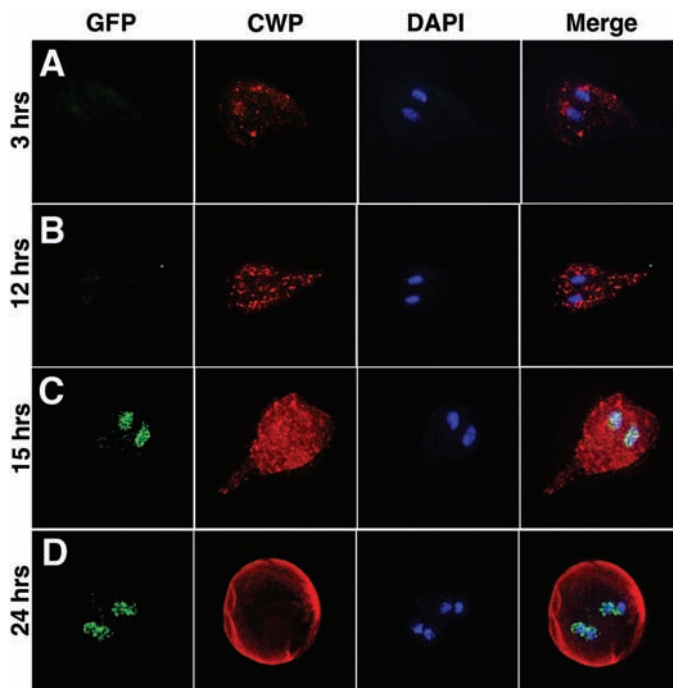
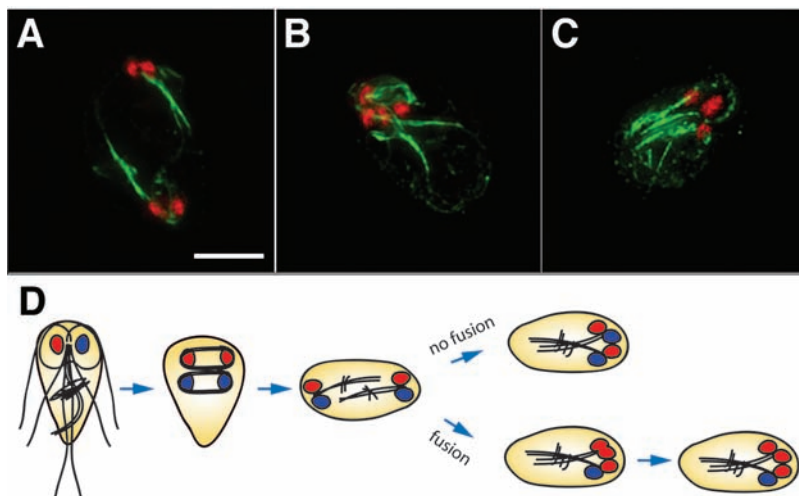


**Fig. 3.** The microtubule cytoskeleton in cysts and a model of nuclear movement. (A to C) Encysting cells were immunolabeled with antibodies to  $\alpha$ -tubulin (green) and the DNA stained with DAPI (false color, red). (A) Two pairs of nuclei are at opposite ends of the cell. (B) Four nuclei clustered together at one end of the cell. (C) Only three nuclei are distinguishable in the cluster. Bar, 5  $\mu$ m. Also see movies S4 to S6. (D) A model for plasmid exchange during encystation. A trophozoite has two independently inherited nuclei, blue or red, and only one (red) contains plasmids. Each nucleus divides during encystation, resulting in two pairs of non-daughter nuclei at opposite ends of the cell. After nuclear migration, fusion occurs between non-daughter nuclei (i.e., between a red and a blue nucleus), leading to transfer of genetic material. Subsequently, fused nuclei undergo fission and move apart, resulting in three (red) nuclei containing plasmids.



Downloaded from www.sciencemag.org on March 23, 2008

RecA family member, have been identified (12). Because DMC1B is expressed in vegetatively growing trophozoites and cysts whereas DMC1A is cyst-specific, we postulate that DMC1B may have a Rad51-like function and be involved in somatic DNA damage repair. Similarly, we suspect that although Mnd1 is involved in meiosis-specific recombination in other organisms, it may have a more general role in *Giardia*.

To determine when HOP1::GFP begins to be localized to the cyst nuclei, we monitored encystation over 24 hours with an antibody to cyst wall protein (CWP), which is transported via encystation-specific vesicles (ESVs) to the exterior of the cell and deposited to form the cyst wall (14). Three hours after induction of encystation, CWP was detected in ESVs in the cytoplasm (Fig. 4A), and the number of ESVs continued to increase through the first 12 hours (Fig. 4B). After 15 hours, cells were filled with ESVs, and HOP1::GFP was first detected in the two nuclei of the encysting trophozoite (Fig. 4C). By 24 hours (Fig. 4D), mature cysts with four nuclei and a defined wall were present, and HOP1::GFP was localized to all four nuclei. Thus, HOP1, which is involved in binding double-strand breaks during meiosis in yeast (15), is first detected in the nuclei in *Giardia* during encystation and persists indefinitely in cysts.

Karyogamy during encystation, if accompanied by homologous recombination and/or gene conversion driven by the HMGs, could provide a mechanism by which *Giardia* maintains low levels of allelic heterozygosity. This parasexual process, which we call diplomixis, appears to be unique to *Giardia*, although we predict that it occurs in other members of the order Diplomonadida. Unlike automixis, diplomixis is not accompanied by meiotic genome reduction and the subsequent fusion of gametes from the same parent, as is found in the sexual or parasexual life cycle of other organisms (16). It is also possible that rare meiotic events occur in the wild, as suggested by a recent *Giardia* population study (17). Understanding the functions of the HMGs and the behavior of chromosomes as nuclei fuse will be essential to test for the occurrence of homologous recombination. A deeper understanding of the roles of these genes, as well as others involved in karyogamy, may shed light on the evolution of meiosis and provide new targets for drug treatments.

#### References and Notes

1. L. Savioli, H. Smith, A. Thompson, *Trends Parasitol.* **22**, 203 (2006).
2. R. D. Adam, T. E. Nash, T. E. Wellems, *Nucleic Acids Res.* **16**, 4555 (1988).
3. K. S. Kabnick, D. A. Peattie, *J. Cell Sci.* **95**, 353 (1990).

4. L. Z. Yu, C. W. Birky, R. D. Adam, *Eukaryot. Cell* **1**, 191 (2002).
5. H. G. Morrison *et al.*, *Science* **317**, 1921 (2007).
6. S. Teodorovic, J. M. Braverman, H. G. Elmdendorf, *Eukaryot. Cell* **6**, 1421 (2007).
7. R. D. Adam, *Clin. Microbiol. Rev.* **14**, 447 (2001).
8. R. Bernander, J. E. Palm, S. G. Svärd, *Cell. Microbiol.* **3**, 55 (2001).
9. M. S. Sagolla, S. C. Dawson, J. J. Mancuso, W. Z. Cande, *J. Cell Sci.* **119**, 4889 (2006).
10. C. W. Birky, *Genetics* **144**, 427 (1996).
11. Materials and methods are available as supporting material on Science Online.
12. M. A. Ramesh, S. B. Malik, J. M. Logsdon, *Curr. Biol.* **15**, 185 (2005).
13. A. M. Villeneuve, K. J. Hillers, *Cell* **106**, 647 (2001).
14. D. S. Reiner, H. Douglas, F. D. Gillin, *Infect. Immun.* **57**, 963 (1989).
15. N. M. Hollingsworth, L. Goetsch, B. Byers, *Cell* **61**, 73 (1990).
16. A. S. Kondrashov, *Annu. Rev. Ecol. Syst.* **28**, 391 (1997).
17. M. A. Cooper, R. D. Adam, M. Worobey, C. R. Sterling, *Curr. Biol.* **17**, 1984 (2007).
18. We thank the Cande and Dawson labs for discussion, as well as E. Slawson for help with experiments. We gratefully acknowledge funding from the NIH (grants A1054693 to W.Z.C. and 1F32GM078971 to M.K.P.) and the NSF (predoctoral fellowship to M.L.C.).

#### Supporting Online Material

www.sciencemag.org/cgi/content/full/319/5869/1530/DC1  
Materials and Methods

Figs. S1 and S2

References

Movies S1 to S6

4 December 2007; accepted 11 February 2008

10.1126/science.1153752

## Direct Visualization of Horizontal Gene Transfer

Ana Babić,<sup>1,2\*</sup> Ariel B. Lindner,<sup>1,2</sup> Marin Vulić,<sup>1,2†</sup> Eric J. Stewart,<sup>1,2†</sup> Miroslav Radman<sup>1,2,3‡</sup>

Conjugation allows bacteria to acquire genes for antibiotic resistance, novel virulence attributes, and alternative metabolic pathways. Using a fluorescent protein fusion, SeqA-YFP, we have visualized this process in real time and in single cells of *Escherichia coli*. We found that the F pilus mediates DNA transfer at considerable cell-to-cell distances. Integration of transferred DNA by recombination occurred in up to 96% of recipients; in the remaining cells, the transferred DNA was fully degraded by the RecBCD helicase/nuclease. The acquired integrated DNA was tracked through successive replication rounds and was found to occasionally split and segregate with different chromosomes, leading to the inheritance of different gene clusters within the cell lineage. The incidence of DNA splitting corresponds to about one crossover per cell generation.

Together with transformation and phage-mediated transduction, conjugation is a key mechanism for horizontal gene transfer in bacteria (1). The first evidence for sex by conjugation in *E. coli* was provided by Lederberg, who obtained prototrophic progeny by mixing two different auxotrophic parents (2). Since then, the phenomenon of horizontal gene transfer has been shown to be responsible for widespread transfer among bacterial populations of genes conferring antibiotic resistance, metabolic functions, and virulence determinants.

Conjugational DNA transfer is driven by the F plasmid unidirectionally from an F<sup>+</sup> donor cell to an F<sup>-</sup> recipient cell. The F plasmid contains all the genes required for conjugation (e.g., mediat-

ing the contact between donor and recipient cells) and for regulation of DNA mobilization and its unidirectional transfer (3). At low frequencies, the F plasmid can integrate into the chromosome of the host cell, giving rise to an Hfr (high frequency of recombination) strain (4). Chromosomal genes of the Hfr bacterium can be mobilized and transferred to a recipient. In some cases, F can excise from the chromosome of Hfr, creating an F' molecule that carries chromosomal genes as well as the conjugation genes (5). Both Hfr and F' can serve as DNA vehicles in horizontal gene transfer between bacteria.

The contact between mating cells is mediated by a tube-like structure known as the F pilus (3). DNA is transferred from the donor to the recip-

ient in single-stranded form and converted to duplex DNA by the synthesis of the complementary strand in the recipient cell. Once the conjugational transfer ceases, double-stranded donor DNA is either circularized (in the case of F' transfer) or, in the case of Hfr transfer, incorporated into the recipient chromosome by RecA-dependent homologous recombination or degraded by RecBCD exonuclease (3, 6).

Many aspects of the mechanism and consequences of conjugation remain unresolved, including the role of the F pilus in DNA transfer during conjugation, the fate of the transferred DNA, the global frequency of the horizontal gene transfer (versus the frequency of inheritance of individual genetic markers), and the pattern of inheritance of donor DNA present in the initial transconjugant cell. To address these questions, we have developed an experimental system that enables us to distinguish the transferred donor DNA from both donor and recipient DNA, and to visualize DNA transfer and recombination by means of fluorescence microscopy in real time,

<sup>1</sup>INSERM U571, Paris F-75015, France. <sup>2</sup>Université Paris Descartes Faculté de Médecine, Paris F-75015, France. <sup>3</sup>Mediterranean Institute for Life Sciences, Meštrovićevo Šetalište bb, 21000 Split, Croatia.

\*Present address: Unité Plasticité du Génome Bactérien, CNRS URA 2171, Institut Pasteur, 25 rue de Dr. Roux, Paris 75724, France.

†Present address: Department of Biology, Northeastern University, 309 Mugar Hall, 360 Huntington Avenue, Boston, MA 02115, USA.

‡To whom correspondence should be addressed. E-mail: radman@necker.fr